SUBSURFACE PROCESSES LAB

UNIVERSITY of CALIFORNIA IRVINE

Proppant distribution in a fracture subjected to normal stress:
Formation of sand-fiber islands capable of supporting an applied load

Ricardo Medina[1], Russell Detwiler[1], Romain Prioul[2], Wenyue Xu[2], J. Alberto Ortega[3]
[1]Civil and Environmental Engineering, University of California, Irvine; [2]Schlumberger-Doll Research, Cambridge, MA; [3]Schlumberger, Sugar Land, TX

Schlumberger

MR41A-2617

Introduction

During the shut-in stage of hydraulic fracturing, fracture aperture decreases, which traps proppant between the fracture walls. The resulting proppant distribution determines the hydraulic conductivity of the fracture. If proppant is uniformly distributed throughout the fracture, proppant permeability will dictate the resulting fracture conductivity. However, if proppant is distributed in isolated islands surrounded by proppant-free regions, conductivity may be enhanced. Optimizing the creation of such islands requires a quantitative understanding of the factors (i.e. normal stress, solid volume fraction, carrier fluid composition, etc) that control the spatial distribution of proppant within the fracture as well as its evolution during closure. We carried out a set of experiments to characterize the spatial and temporal distribution of proppant settling inside a transparent fracture. Upon initial filling, the proppant is allowed to settle for 25 minutes before applying a normal stress. Adding polymeric fibers drives the formation of fiber-solid regions that can support the applied normal stress and prevent fracture closue. The formed fiber-sand islands have a solid content, ϕ, larger than the random loose packing limit (ϕ=0.55), despite the relatively low solid content of the bulk initial mixture (ϕ=0.17)

Uniform applied normal stress fracture: experimental setup

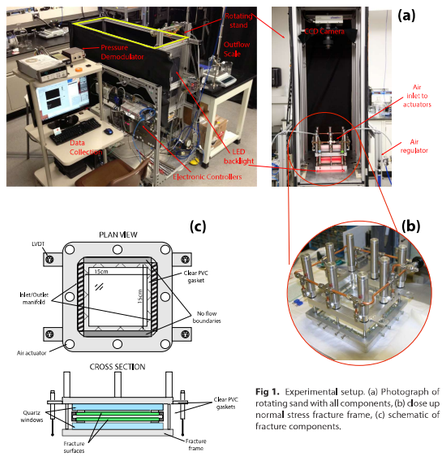

Fig 1. Experimental setup. (a) Photograph of rotating sand with all components, (b) close up normal stress fracture frame, (c) schematic of fracture components.

Our transparent fracture is composed of two 15 x 15 x 1.2 cm flat pieces of glass which are sealed by four manifolds (two no-flow, one inlet, and one outlet manifold). The fracture is secured inside the aluminum frames with fused-quartz windows by placing one clear PVC-gasket on the top and bottom of the fracture. Eight reverse action pneumatic-actuators are mounted on the top plate of the aluminum frame, the steel rods securely screw to the bottom frame. Air pressure activates the actuators, the rods retrieve into the actuator cylinder and cause the two aluminum frames to collapse - forcing fracture closure. Four linear variable displacement transducers (LVDT) measure the displacemtent of the fracture. The fracture assemply is rigidly mounted to a rotating stand equipped with a high resolution CCD camera, a LED backlight, and electronic controllers.

Applied-normal-stress system characterization

The response of actuators to an applied air pressure was independently measured for each of the eight actuators. Fig. 2, demonstrates that all actuators have very similar response to the applied air pressure.

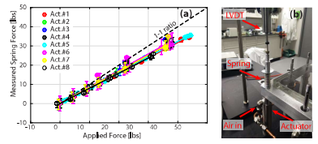

Fig 2. (a) Independent measure of the response of each actuator to applied force, (b) Air pressure activates actuator while an LVDT measures displacement; calculated applied force is compared to compression force of the spring (k_s=311.7lbs/in).

The fracture was filled with water, sealed with no-flow manifolds, and the fracture pore pressure was measured as the applied normal stress was increased. Pore pressure almost matched the measured normal stress. The difference between pore pressure and normal stress, Fig. 3, is due to shear stress generated by the glass side contacting the gaskets that seal the fracture.

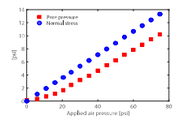

Fig 3. Measured fracture pore pressure and normal stress as applied air pressure increases. The difference is attributed to shear stresses between glass and gaskets.

Experiments in transparent analog fractures allow direct measurement of fracture aperture and solids distribution

Light transmission techniques allow accurate measurement of the fracture aperture field, b_{ij}. Beer-Lambert law is used to calculate the absorbace field (A_{ij}) which is used to calculate the aperture field [Detwiler, et al., 1999].

$$I = I_0 e^{-\mu C b} \quad (1)$$

$$A = ln\left(\frac{I_{clear}}{I_{dye}}\right) = \mu(C_d - C_c)b \quad (2)$$

$$b_{ij} = \frac{A}{\langle A \rangle}\langle b \rangle \quad (3)$$

where
A = absorbance
C_c = solute concentration (dye)
C_d = solute concentration (Dil water)
b = aperture
I = Irradiance
I_0 = Source irradiance
I_{clear} = Irradiance of clear/dyed solution
μ = solute attenuation coeff.

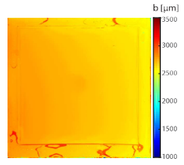

Fig 4. Measured fracture aperture field. Mean aperture, <b> = 2697.0 μm, σ = 78.3 μm.

An independent test inside a constant-aperture fracture was conducted to measure light absorbance by a sand-filled fracture at a known solid volume fraction. A slurry mixture was prepared with ϕ_o=0.5 (40/70 mesh sand) and injected into the fracture. Sand was allowed to settle, undisturbed, for six days. We derived a linear relationship between solid volume fraction (ϕ) and the measured absorbace (A), following the absorption and scattering theory described by Bohren and Huffman (1983).

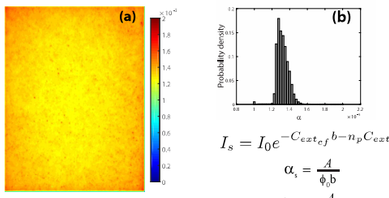

Fig 5. (a) Measure of α-field for sand-filled settled fracture and (b) probability density of measured α-field.

$$I_s = I_0 e^{-C_{ext_f} b - n_p C_{ext_s} b} \quad (4)$$

$$\alpha_s = \frac{A}{\phi_s b} \quad (5)$$

$$\phi_{s_t} = \frac{A_t}{\alpha_s b_t} \quad (6)$$

where
n_p = particle density (# particles/unit vol.)
ϕ = solid volume fraction
α = light-absorbance per unit length
C_{ext_f} = extinction cross-section of carrier fluid (light attenuation)
C_{ext_s} = extinction cross-section of sand (light attenuation)
subscripts s and f denote sand and time, respectively

Creation of fiber-proppant islands that can sustain applied-normal-stress and keep fracture open

Proppant fluid and experimental procedure

The slurry was prepared by mixing 0.48% guar gum and water, which produced a shear thinning fluid with an apparent viscosity of μ= 1.2 Pa•s at a shear rate of γ=0.1s^{-1}. We used a rotary paddle to mix in silica sand (40/70 mesh) and polymeric fibers with large aspect ratio (A_r = l/d ≈ 500) to produce the slurry. Upon mixing, the slurry was immediately transferred to a pneumatic tank and injected into the fracture until ~10 fracture volumes had passed through the system. For the zero-applied-normal-stress experiment (Test A) we allowed solids to settle for approximately 2 hours (previously conducted experiments in a constant-aperture fracture demonstrated negligible settling or solid distribution changes after ~1.5 hours). After two hours we injected solids-free carrier fluid for up to 25 fracture volumes. For the applied-normal-stress experiments we allowed the proppant to settle for ~25 minutes before applying the first normal stress: we applied a normal stress at regular time intervals of ~50 minutes increasing by 1.8 psi normal stress (i.e. increasing air pressure by 10 psi) to a maximum of 12.8 psi.

Solid Volume Fraction (ϕ)
ϕ_{total} = 0.172
ϕ_{sand} = 0.168
ϕ_{fiber} = 0.004

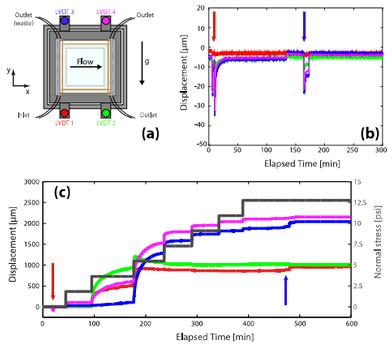

Fig 6. Experimental setup (a) and measured LVDT displacement for (b) experiment with zero-applied-normal-stress (b) and with applied-normal-stress (c). Color of displacement data corresponds to the colors indicated for each LVDT. Positive displacement indicates fracture aperture reduction. Red arrows indicates slurry injection and blue arrows indicate solids-free carrier fluid injection (flowback).

The displacement data for Test A (Fig. 6b) shows that the fracture opened slightly as fluid was injected into the fracture; however, the fracture returned to its original state (± 3μm) after the flow stopped. This and previous experiments show that fiber-sand islands developed early on in the settling process and remained suspended thoughout the duration of the experiment. However, these fiber-sand islands (along with much of the solids) are flushed out of the fracture once solids-free carrier fluid was injected. In contrast, recorded LVDT displacements for the applied-normal-stress experiments show that fracture aperture can reduce up to ~85% on the top regions, due to the absence of solids which have migrated (settled). The bottom regions of the fracture, where solids have settled, experience an aperture reduction of only ~40% at the maximum applied stress. As the normal stress increased, the fracture aperture reduced and fiber-sand islands that formed at early times get compressed, therefore increasing ϕ at the local scale. Additionally, the initial solid distribution of all experiments (top row of Fig. 7) demonstrate the reproducibility of our experimental procedure.

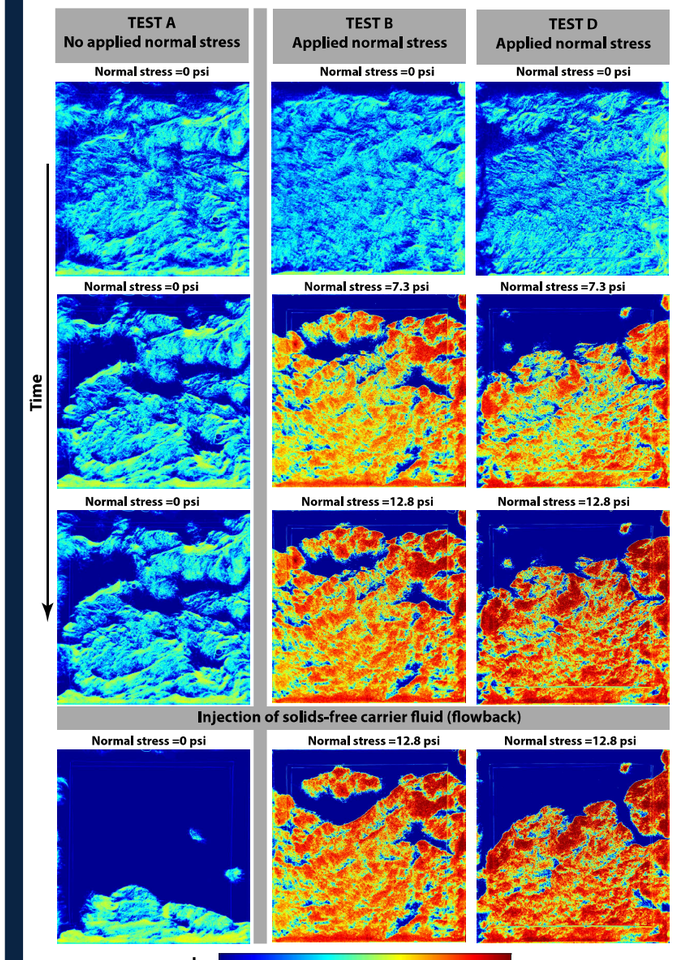

Fig 7. Solid volume fraction distribution for Test A (left column), Test B (middle column), and Test D (right column). Proppant in Test A was allowed to settle without an applied normal stress, for approximately 2.5 hours before the flowback experiment was conducted. Test B and Test D were allowed to settle for ~25 minutes before the normal stress was applied; after that, we increased the applied normal stress in regular increments of 1.8 psi up to a maximum normal stress of 12.8 psi every ~50 minutes.

Spatial distribution of load-bearing proppant-fiber islands

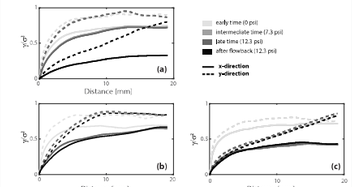

Fig 8. Normalized variograms for (a)Test A, (b) Test B, and (c) Test D. Different times correspond to the frames shown in Fig. 7.

Without applied-normal-stress (Test A), the proppant distribution varied by a small amount over time (light gray to dark gray). After the solids were carried out of the fracture (flowback) there was a perceptible change in the spatial distribution of solids. Therefore, differences in spatial statistics for Test B and D can be directly related to the increased normal-stress applied to the system. Variograms for Test B and D show only minimal changes after flowback (black lines). All cases showed a pronounced anisotropy, due to the increasing size of the individual sand-fiber islands. As the applied stress increased the correlation length increased, which is due to the initial orientation of the fiber networks in the flow direction.

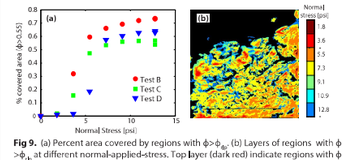

Fig 9. (a) Percent area covered by regions with $\phi > \phi_{lb}$, (b) Layers of regions with ϕ >ϕ_{ub} at different normal-applied-stress. Top layer (dark red) indicate regions with ϕ >ϕ_{ub} after the first load application. The bottom layer (blue) regions were formed (i.e. compacted) at the last normal-stress application.

We use ϕ_{lb}=0.55 (the random loose packing limit) as the minimum ϕ that can support an external load [Onoda & Liniger, 1990]. Applying image processing techniques on the ϕ-field, we calculated the extent of regions with ϕ>ϕ_{ub}. As the normal stress was increased the total area covered these regions increased, as the fiber-sand islands compacted and spread.

Conclusions

- The applied-normal-stress system we have developed yields reproducible initial proppant distribution within the fracture.
- Adding fibers to hydraulic fracturing fluids, even at low concentrations, forms fiber-sand islands with ϕ significantly higher than the solid content of the mixture ($\phi_{islands} > \phi_{tot}$).
- Sand-fiber islands support the applied-normal-stress and prevent full fracture closure.
- After injecting solids-free carrier fluid some solids are washed away, creating connected pathways around the sand-fiber islands.

Bohren, CF & Huffman, DR. Absorption and scattering of light by small particles. Wiley, New York, 1983.
Detwiler, et al. *Water Res. Research*. 1999, **35**(9) 2605-2617.
Onoda, GY & Liniger, EG. *Phys Rev. Lett.* 1990, **64**(22) 2727-2730.